Z. Phys. C – Particles and Fields 44, 385–392 (1989)

Zeitschrift für Physik C Particles and Fields

Field distortions from persistent currents in the superconducting HERA magnets

H. Brück[1], R. Meinke[1], F. Müller[2], P. Schmüser[2]

[1] Deutsches Elektronen-Synchrotron DESY, D-2000 Hamburg 52, Federal Republic of Germany
[2] II. Institut für Experimentalphysik der Universität, D-2000 Hamburg 50, Federal Republic of Germany

Received 23 March 1989

Abstract. Measurements and calculations are presented on the sextupole and decapole components in the HERA dipole magnets and the 12-pole and 20-pole components in the quadrupoles. The data show a strong current dependence and a characteristic hysteresis behaviour. Good agreement is found with model calculations which are based on eddy currents in the niobium-titanium filaments of the superconducting cable.

1 Introduction

The proton storage ring of the proton–electron collider HERA [1] is equipped with superconducting dipole and quadrupole magnets. For the nominal energy of 820 GeV the necessary dipole fields of 4.68 T and quadrupole gradients of 91.2 T/m are achieved with a current of 5027 A in the coils. At low excitation, the superconducting magnets suffer from severe field distortions caused by persistent eddy currents in the superconductor which are induced when the main field is increased or decreased. Contrary to the situation in normal magnets the eddy currents do not decay exponentially but continue to flow forever, except for a slight logarithmic time dependence [2, 3]. One of the unfortunate consequences is the well-known sextupole field observed in all superconducting dipoles but in the HERA magnets – owing to the low proton injection energy of 40 GeV – additional higher multipoles are important: a decapole (10-pole) in the dipole and a dodecapole (12-pole) in the quadrupole.

At the injection energy, corresponding to a magnet current of 245 A, the sextupole component is an order of magnitude larger than tolerable and has to be compensated by means of sextupole correction coils [4]. But also the 10-pole and 12-pole fields require a compensation by special correction coils to avoid a sizable reduction in the dynamic aperture of the HERA machine [5].

A precise knowledge of the eddy current fields is indispensable to enable appropriate correction mechanisms during the injection and initial acceleration of the proton beam. The sextupoles are particularly important since they influence the chromaticity of the machine. For this reason, detailed measurements are performed on each magnet before installation in the ring. A theoretical understanding is needed as well because the field distortions depend on several parameters like the helium temperature and the previous current cycling which may be different in the test facility and in the accelerator.

A computer program for the calculation of multipole fields generated by persistent eddy currents was developed by Green [6] at LBL and applied to a variety of superconducting accelerator magnets, including the HERA dipole [7]. A similar program was written by Duchateau [8] at SATURNE and used by Perot [9] to predict the multipoles in the warm iron dipoles which were originally proposed for UNK and HERA. Both programs reproduce the main features of the multipole fields quite well. In order to gain detailed insight into the properties of our dipole and quadrupole magnets at various operating conditions as well as of the beam pipe correction coils we have developed an own computer code, following the general outline presented in [6].

The measurement technique and results of multipole measurements in the HERA dipole and quadrupole magnets are described in Sect. 2. The physical model of the eddy current effects and the method of calculation as well as a comparison between data and model predictions are presented in Sect. 3. A summary is given in Sect. 4.

2 Method of multipole measurements

The field of a superconducting accelerator magnet is conveniently expressed in terms of a multipole expan-

sion (see e.g. [2]). Taking the beam direction as the z axis of a cylindrical coordinate system (r, θ, z) the general expressions for the azimuthal and radial field components read

$$B_\theta(r,\theta) = B_{\text{ref}} \sum_{n=1}^{\infty} \left(\frac{r}{r_0}\right)^{n-1} (b_n \cos(n\theta) + a_n \sin(n\theta))$$

$$B_r(r,\theta) = B_{\text{ref}} \sum_{n=1}^{\infty} \left(\frac{r}{r_0}\right)^{n-1} (-a_n \cos(n\theta) + b_n \sin(n\theta)).$$

Here r_0 is the reference radius of the expansion which is chosen to be 25 mm for the HERA magnets, i.e. 2/3 of the inner coil radius. The b_n and a_n are the normal and skew multipole coefficients. B_{ref} is a reference field, measured in Tesla, which depends on the type of magnet. For dipole magnets, B_{ref} is chosen to be the dipole field itself whereas for quadrupoles the product of the gradient g and the reference radius r_0 is taken. With this convention, $b_1 = 1$ for an ideal dipole and all other coefficients vanish; similarly, for an ideal quadrupole $b_2 = 1$ and all other b_n and a_n are zero. Real magnets have of course non-vanishing higher multipole components due to mechanical imperfections, but the quality requirements are stringent for magnets to be used in a storage ring with beam lifetimes of many hours. For HERA the tolerance on the normal sextupole in the dipole magnets is $4 \cdot 10^{-4}$ and about $1 \cdot 10^{-4}$ for most of the remaining higher-order multipole components. The corresponding limits are $3 \cdot 10^{-4}$ for the quadrupole magnets which contribute less to the overall accelerator field since they are shorter, weaker and less numerous than the dipoles.

The HERA magnets have an inner coil diameter of 75 mm and are equipped with a cold beam pipe with

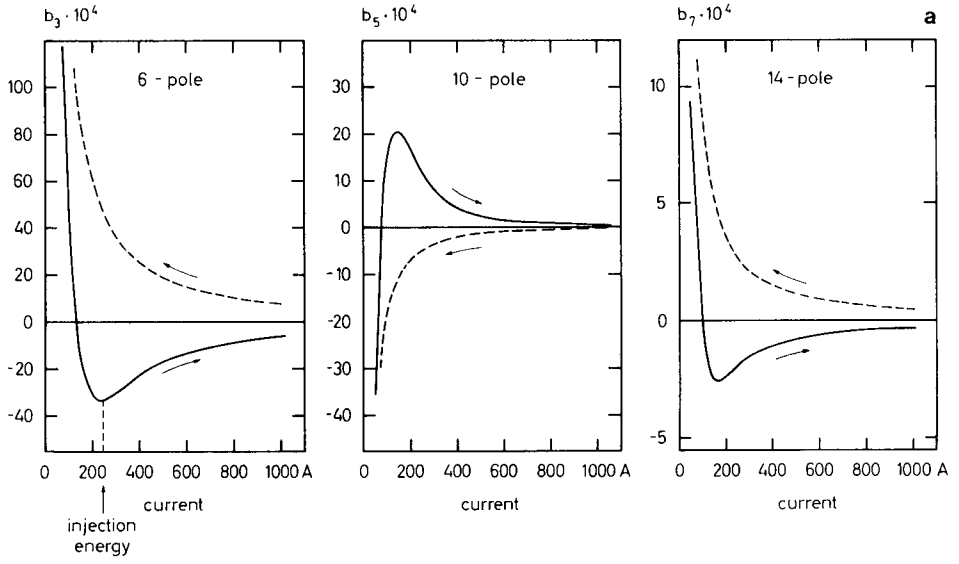

Fig. 1. a Current dependence of the 6-, 10- and 14-pole coefficients of a HERA dipole. Following an initial current cycle 0 A → 6000 A → 50 A, the current is increased to 6000 A (continuous curves) and then decreased to 50 A again (dashed curves). **b** Current dependence of the 12- and 20-pole coefficients of a HERA quadrupole

an inner diameter of 55 mm. On the cryogenic test stands, a 45 mm diameter titanium tube, surrounded by superinsulation, is mounted inside the evacuated beam pipe.

The multipole coefficients of the magnets are measured using rotating pick-up coils [10] at room temperature. The induced voltage is digitized with a voltage-to-frequency converter and is summed in an up-down counter [11] whose contents is read out at 128 equally spaced angular steps each revolution.

For the dipole magnets, pick-up coils with a length of 2.4 m are used. To cover the entire magnetic length of 8.8 m the measurements are performed in four longitudinal positions. In the following we use only the data from the first position where no sextupole and quadrupole correction coils are mounted on the beam pipe. These correction coils have a sizable influence on the persistent current fields, but this effect will be analysed elsewhere.

The quadrupole magnets are measured with a 1.1 m long pick-up coil. The total magnetic length of about 1.9 m is covered with two longitudinal positions. In this case the multipole data integrated over the full length can be used.

The pick-up coils for the measurements of dipole and quadrupole magnets are designed to cancel the induction resulting from the main poles which are typically four orders of magnitude larger than the disturbing higher-order poles. With this technique an accuracy of $1\text{–}2 \cdot 10^{-5}$ relative to the main poles is achieved.

The measured 6-, 10- and 14-pole coefficients of a HERA dipole and the 12- and 20-pole coefficients of a quadrupole are plotted in Figs. 1a,1b as a function of the magnet current. One observes a strong current dependence and a distinct hysteresis behaviour. For increasing currents the multipole coefficients follow the "up-ramp" curve while for decreasing currents the "down-ramp" curve is measured. Assuming that induced eddy currents in the superconductor are the source of the disturbing multipole fields, the hysteresis can be understood qualitatively since these currents change their sense of rotation when the ramp direction of the main field is reversed. For a quantitative understanding of this effect a detailed physical model is needed. In particular, the observation that the multipole coefficients change their sign on the "up-ramp" branch has to be explained.

The persistent currents depend critically on the previous history of the current in the magnet and also on effects like the power supply regulation and overshoots of the current during the ramping process. Good reproducibility is obtained if a current cycle $0\,A \rightarrow 6000\,A \rightarrow 50\,A$ with a ramp rate of 10–20 A/s is performed before starting a hysteresis measurement. Between successive data points, the magnet current is changed with a speed of 10 A/s. On each of the branches of the hysteresis curve, the current has to be varied monotonically, strictly avoiding a sign reversal of DI/dt.

3 Calculation of persistent eddy currents and of the resulting multipole fields

Cross sections of the HERA dipole [12] and quadrupole [13] are shown in Fig. 2a,b. Both coil types are wound from a keystoned Rutherford-type cable with 24 strands in the dipole and 23 strands in the quadrupole. Half of the dipoles are produced in Italy with LMI superconductor, the other half in Germany with ABB conductor. The quadrupole production is split between France and Germany but all coils are made

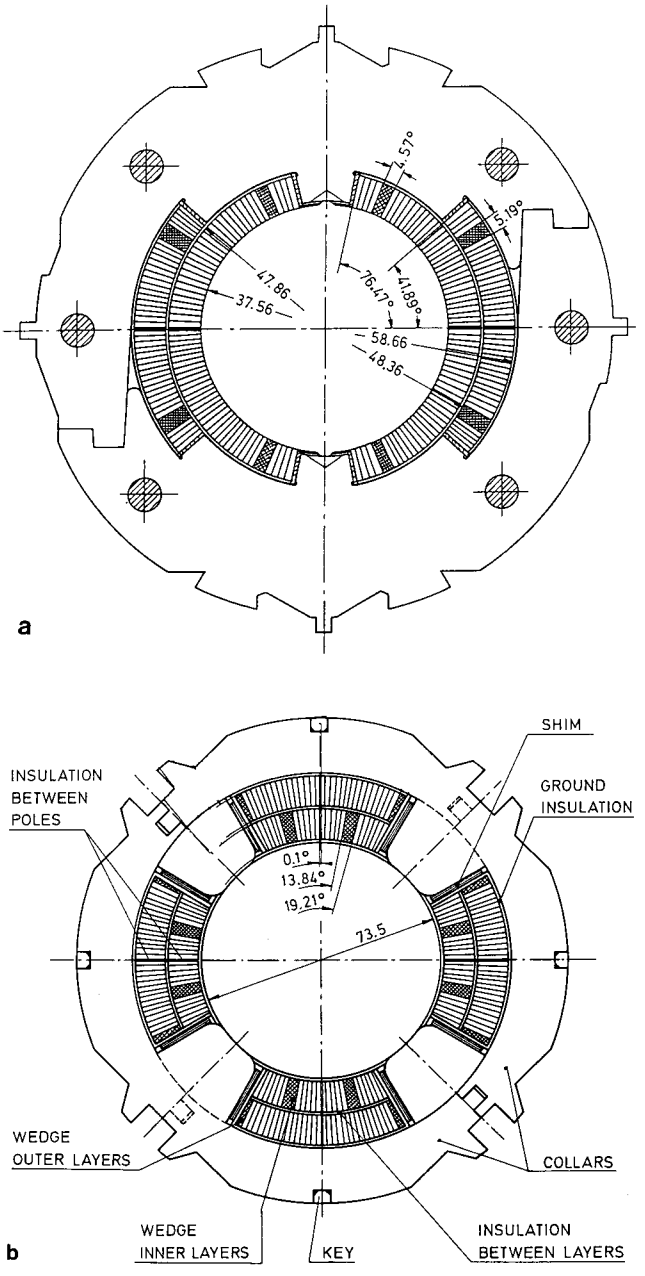

Fig. 2. a Cross section of the HERA dipole coil. The coil is clamped with aluminum collars and surrounded by a cold iron yoke with an inner bore radius of 88.4 mm. **b** Cross section of the HERA quadrupole coil. The collars are made of stainless steel and are surrounded by a cold iron yoke with an inner radius of 78 mm

Table 1. Parameters of the superconducting cables

	ABB Dipole cable	LMI Dipole cable	VAC Quadrupole cable
Strand diameter/mm	0.84	0.84	0.84
Filament number	1230	900	636
Filament diameter/μm	14	16	19
Cu:NbTi ratio	1.8	1.8	1.8
Twist pitch/mm	25	25	25
Number of strands per cable	24	24	23
Cable pitch/mm	95	95	95
Average critical current at 5.5 T 4.6 K	8870 ± 220 A	8320 ± 330A	8030 ± 90A

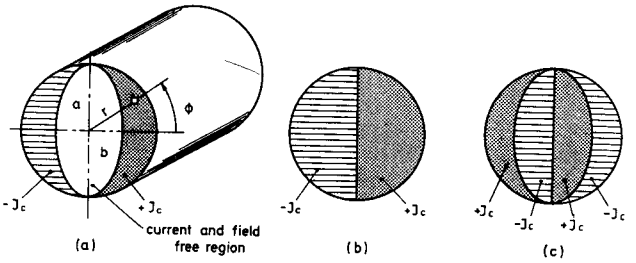

Fig. 3. Schematic view of the persistent eddy currents which are induced in a superconducting filament by a time dependent external field. **a** The external field in raised from zero to a value B_e less than the penetrating field B_p. **b** A "fully penetrated" filament, i.e. $B_e \geqq B_p$. **c** Current distribution which results when the external field is first increased from zero to a value above B_p and then decreased again

from Vacuumschmelze conductor. The parameters of the superconductors are summarized in Table 1.

The program to compute the fields of persistent eddy currents in dipole and quadrupole magnets consists of three parts:

In the first step the main field, generated by the transport current in the coil, is calculated within the useful aperture of the magnet but also at any place inside the coil windings. A knowledge of this field is necessary since it is the time variation of just this "local" field which induces the eddy currents in the superconductor. The field calculation can be done analytically with good accuracy and will not be described here. Details can be found in [2].

In the second step, the eddy current pattern is computed. An essential feature of twisted multifilamentary superconductors is the fact that long-lasting eddy currents occur only within single filaments and not between different filaments of a strand or between different strands of a transposed cable. The eddy current distribution within individual filaments is computed from the time dependence of the local field, taking into account the previous history of the current distribution in the filament.

In the last step, the field generated by a representative number of filaments is calculated. For simplicity, the vector potential is used instead of the magnetic field vector and the symmetries of the coil are taken into consideration.

In the treatment of eddy currents we follow Wilson's analysis [14] of time varying fields in type II superconductors. The eddy currents which are induced between different filaments of a twisted multifilamentary conductor decay exponentially with a time constant [14]

$$\tau = \frac{\mu_0}{2\rho}\left(\frac{L}{2\pi}\right)^2, \tag{2}$$

Here ρ is the resistivity of the copper matrix and L the twist length. For the HERA conductors with $L = 25$ mm we estimate a decay time of less than 0.1 s. In the Rutherford-type cables as used in our magnets also the eddy currents between different strands decay so rapidly that they have no influence on the multipole measurements.*

Persistent eddy currents exist therefore only within single filaments, provided the filament spacing is large enough like in our cable that proximity-coupling effects [16] can be neglected. To calculate these currents we use the experimentally verified "critical state" model [17]. According to this model, a type II superconductor tries to expel any external field change by generating a bipolar current distribution with the highest possible density, namely the critical current density $J_c(B, T)$ at the given local field and temperature. Since the local field can be considered as homogeneous on the scale of a filament diameter (10–20 μm) the resulting current pattern in the filament can be computed analytically with good accuracy.

In the following, we distinguish between the "external" field B_e, i.e. the field which induces the eddy currents in the filament and is identical to the local field mentioned above, and the "internal" field B_i which is generated by those eddy currents. Suppose the external field is increased from zero to a small value B_e. The induced current has to follow a $\cos\theta$-like distribution to generate a homogeneous inner field B_i which just cancels the external field in the current-free region of the filament (see Fig. 3a). This region can be approximated by an ellipse with large half axis $a = r_f$ (filament radius), small half axis b and eccentricity $e = b/a$. The field inside the ellipse, generated by the eddy currents, is found by simple integration

$$B_i = -\frac{2\mu_0 J_c a}{\pi}\left(1 - e\frac{\arcsin\sqrt{1-e^2}}{\sqrt{1-e^2}}\right). \tag{3}$$

From the condition $B_i = -B_e$ one determines the eccentricity e as a function of the external field B_e. The highest field which can be shielded from the interior of the filament is called the "penetrating" field B_p and is

* Eddy currents with a fast time dependence are discussed in a recent paper by ter Avest and van de Klundert [15]

obtained for an ellipse shrunk to a line, i.e. $e = 0$.

$$B_p = \frac{2\mu_0 J_c a}{\pi} \tag{4}$$

Figure 3b shows the currents in the "fully penetrated" filament.

The applied field may be raised to much larger values than B_p which is only about 0.13 T for the HERA conductor. In that case the same current pattern is obtained as in Fig. 3b but the field inside the filament is no more zero.

If now the field is decreased again, eddy currents with opposite polarity are superimposed because the superconductor tries to avoid a change of the inner field. A more complicated current pattern arises as indicated in Fig. 3c.

The eddy current loops are assumed to be closed at the coil ends. The effect of the short coil ends on the integrated multipole fields can be neglected.

The magnetization (magnetic moment per unit volume) of the $\cos\theta$-like current distribution shown in Fig. 3a is easily computed

$$M = -\frac{4}{3\pi}\mu_0 J_c a(1 - e^2). \tag{5}$$

The peak magnetization is obtained for the fully penetrated filament

$$M_p = |M|_{\max} = \frac{4}{3\pi}\mu_0 J_c a. \tag{6}$$

Note that the quantity M_p is not constant but field dependent. It assumes its maximum value for $B_e = B_p$ and decreases proportional to the critical current density $J_c\,(B_e, T)$ when the external field is raised far beyond the penetrating field.

In the presence of a transport current, (3, 4, 5, 6) have to be modified by a factor $(1 - J_t/J_c(B, T))$ since the current density available to the eddy currents is then given by $J_c - J_t$. This correction factor is negligible near the injection field where the transport current density is two orders of magnitude lower than the critical current density but it becomes significant at high excitation of the magnet.

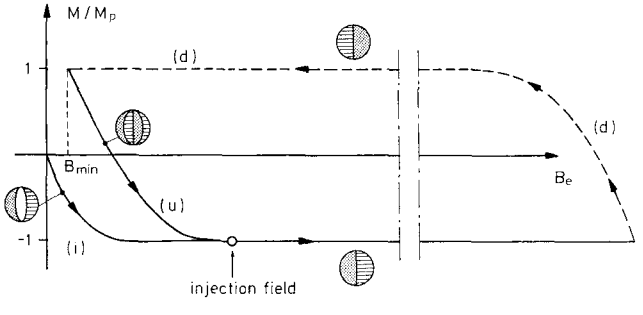

Fig. 4. The normalized magnetization M/M_p of a NbTi filament as a function of the external field. (*i*): initial curve, (*u*): up-ramp branch, (*d*): down-ramp branch. Also shown are the current distributions in the filament

From (3, 5) one can compute the magnetization as a function of the external field. The result is plotted schematically in Fig. 4. We observe a hysteresis behaviour with three different states: Starting at the virgin state the magnetization follows an initial curve (i) and reaches its peak value at $B_e = B_p$. After going up to high fields the ramp direction is reversed and M follows the "down-ramp" branch (d). At a certain minimum current (typically $I_{\min} = 50$ A) the field is increased again and the magnetization follows the "up-ramp" branch (*u*) which has the remarkable feature that M changes its sign from positive to negative values. This is exactly what is observed in the sextupole and dodecapole coefficients (see Fig. 1a,b). Fig. 4 also indicates the current pattern in the filament at different positions of the hysteresis loop.

The calculation of the multipole fields caused by the persistent currents can be performed with similar methods as applied for the main field. The procedure will be described for a dipole only, a generalization to the quadrupole case is straightforward.

For the computation of the main field we consider a conductor at a radius R and an azimuthal angle ϕ, carrying a current $+I$ in the z direction. Due to the symmetry of the dipole coil, there is another conductor with current $+I$ at R and $-\phi$ and two conductors with opposite currents at radius R and angles $\pi \pm \phi$. The vector potential generated by these four currents has only a z component and is given by [2]:

$$A_1(r, \theta) = \frac{2\mu_0 I}{\pi} \sum_{n=1,3,..} \frac{1}{n}\left(\frac{r}{R}\right)^n \cos(n\theta)\cos(n\phi) \tag{7}$$

Only odd multipole orders $n = 1, 3, 5, \ldots$ appear in the expansion.

To generalize this expression for the case of eddy currents we replace the current distribution in each filament by a pair of line currents $+I$ and $-I$ whose strength equals the integrated current density and whose separation d is chosen such that the computed

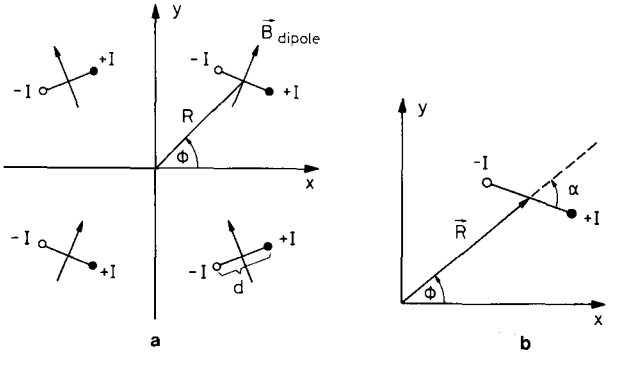

Fig. 5. a Eddy currents induced by the time-dependent main field in four symmetrically arranged filaments inside the dipole coil. The separation d between the positive and negative currents is grossly exaggerated. **b** Definition of the angle α between the line joining the current pair and the position vector **R**

filament magnetization (5) is obtained. (d is about equal to the filament radius). Figure 5a illustrates that the eddy currents obey the same symmetry as the transport current.

For $d \ll R$, the vector potential of the four current pairs in Fig. 5a is given by

$$A_2 \simeq \frac{\partial A_1}{\partial R} \Delta R + \frac{\partial A_1}{\partial \phi} \Delta \phi.$$

With the relations $\Delta R = d \cdot \cos\alpha$, $\Delta \phi = -d \cdot \sin\alpha / R$ (see Fig. 5b for the definition of the angle α) we obtain

$$A_2(r, \theta) = -\frac{2\mu_0 I d}{\pi R} \sum_{n=1,3,..} \left(\frac{r}{R}\right)^n \cos(n\theta) \cos(n\phi + \alpha) \tag{8}$$

The influence of the iron yoke with an inner bore radius R_I is taken into account by the image current method (see e.g. [2]). The image of a current pair at a radius R and angle ϕ appears at $R' = R_I^2/R$ and $\phi' = \phi$. The separation of the image currents is $d' = d \cdot R'/R$ and the angle with respect to the position vector $\mathbf{R}'$ is $\alpha' = \pi - \alpha$. Replacing the quantities R, d, α in (8) by R', d' and α' one gets the iron contribution A_2' to the vector potential. The resulting multipole expansion of the azimuthal field component is then given by

$$\begin{aligned} B_\theta(r, \theta) &= -\frac{\partial}{\partial r}(A_2 + A_2') \\ &= \frac{2(\mu_0 I d)}{\pi R^2} \sum_{n=1,3,..} n \cos(n\theta) \left[\left(\frac{r}{R}\right)^{n-1} \right. \\ &\quad \left. \cos(n\phi + \alpha) - \frac{R}{R'} \left(\frac{r}{R'}\right)^{n-1} \cos(n\phi - \alpha) \right]. \end{aligned} \tag{9}$$

For the product ($\mu_0 I d$) we insert the magnetic moment per unit length derived from (5). Expression (9) has to be summed over all NbTi filaments in one quarter of the dipole coil. Sufficient accuracy is obtained by using one filament for each strand in performing the summation and by multiplying the result with the number of filaments per strand. The multipole coefficients generated by the persistent eddy currents are finally

$$b_n = \left(\sum_{\text{filaments}} B_{\theta,n}(r = r_0, \theta = 0) \right) \Big/ B_0. \tag{10}$$

Here B_0 is the dipole field of the transport current. As for the main field only normal multipoles of the orders $n = 1, 3, 5, \ldots$ occur.

In the quadrupole coil, the persistent eddy currents obey again the same symmetries as the transport current and generate therefore only normal multipoles whose order is an odd multiple of the basic pole order, i.e. the only nonvanishing poles are $b_2, b_6, b_{10}, b_{14}, \ldots$

From the expression (5) of the magnetization it is clear that the magnitude of the multipole fields depends linearly on both the filament diameter $2a$ and the critical current density $J_c(B, T)$ at low field. The critical current density may exceed the transport current density by two orders of magnitude leading to large field distortions in spite of small filament diameters. Unfortunately, critical current data at low fields are not easily accessible. The manufacturers of the HERA superconducting cables measure critical currents only at fields of 5–6 T. No direct measurements exist at the fields of interest. A few superconductor magnetization measurements have been performed by Ghosh and Sampson [18] at BNL on HERA conductors. From these one can derive the critical current density by making use of expression (6) and correcting for the volume fraction of superconductor in the cable.

We have evaluated the BNL measurements on the ABB dipole conductor and have parametrized the critical current density in the following form

$$J_c = 2.3 \cdot 10^{10} \text{A/m}^2 \quad \text{for } B \leqq 0.025\,\text{T}$$

$$J_c(B) = 1.7 \cdot 10^{10} \left(\frac{B}{0.1\,T}\right)^{-0.2} \text{A/m}^2 \quad \text{for}$$

$$0.025\,\text{T} < B \leqq 0.25\,\text{T}$$

$$J_c(B) = 1.5 \cdot 10^{10} \left(\frac{B}{0.25\,\text{T}}\right)^{-0.5} \text{A/m}^2 \quad \text{for } B > 0.25\,\text{T}$$

The numbers refer to a helium temperature of 4.6 K.

We estimate an uncertainty of 10–20% in our knowledge of critical current data at low fields. This is at present the largest source of uncertainty in the calculation of persistent current multipoles. The filament diameter is known to about 5%.

It should be emphasized that no effort has been made to adjust these quantities such that the calculated field distortions fit our data and that no free parameters are present in the model. However, additional magnetization measurements would be highly desirable.

The multipole data measured for a selected dipole magnet (serial number BL537) at a large number of current values between 50 A and 750 A are plotted in Fig. 6. The sextupole and decapole coefficients show a smooth current dependence on both hysteresis branches. Very good reproducibility ($2 \cdot 10^{-5}$) is found when the measurement is repeated. Due to time limitations the majority of the magnets are measured only at a few selected currents. The average data of 19 dipoles are also plotted in Fig. 6, together with their rms standard deviations. These data have been collected over a period of 4 months and agree very well with the recent data of dipole BL537.

Also shown in Fig. 6 are the predictions of the eddy current model. The agreement with the data both in curve shape and absolute magnitude is very good considering the uncertainties in the critical current density mentioned above. Only on the down-ramp branch of the decapole coefficient there is some discrepancy between the measured and calculated

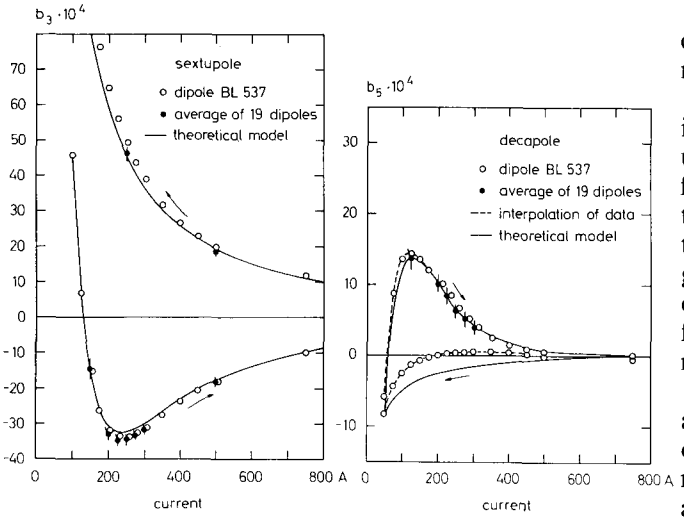

Fig. 6. Measured multipole coefficients of a single dipole and the average coefficients of 19 dipoles plotted against the current in the coil. The magnets were cooled by single-phase helium in forced flow with a temperature of about 4.6 K. Continuous curves: predictions of the eddy current model

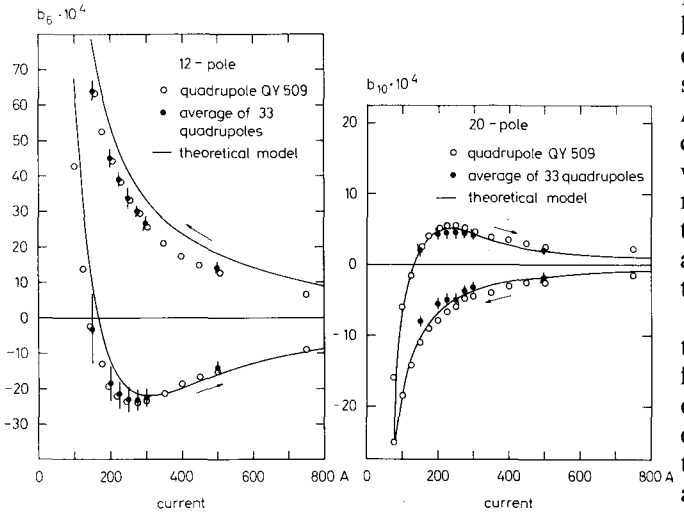

Fig. 7. Measured multipole coefficients of a single quadrupole and the average coefficients of 33 quadrupoles. Continuous curves: predictions of the eddy current model

values. During the accelerator operation the up-ramp branch will be used.

In Fig. 7 we present the multipole data of a single quadrupole (QY 509) and the average data of 33 quadrupoles. Again the measurements reveal good internal consistency and reproducibility. The theoretical curves provide a good description also in this case, but somewhat larger differences are observed on the down-ramp branch of the 12-pole coefficient.

Due to the lack of critical current data for the quadrupole conductor we have used the parametrization made for the ABB conductor which probably overestimates the current density in the VAC conductor by about 5%.

We want to emphasize again, that the theoretical curves shown are absolute predictions and no parameter has been adjusted to yield a good fit to the data.

The persistent currents have also a significant influence on the main field of the magnets. On the up-ramp branch the field is lowered as may be expected from Lenz's rule. For the injection energy of 40 GeV the model predicts a relative reduction of $4 \cdot 10^{-3}$ in the dipole field and of about $3 \cdot 10^{-3}$ in the quadrupole gradient. Precision measurements of the main field component in the magnets have just been started. The first preliminary results are in accordance with the model predictions.

It should be mentioned that the model cannot account for the experimentally observed time dependence [2, 3] of the "persistent" current effects. The measurements presented here were taken immediately after a specific current was reached and are therefore influenced very little by a time variation of the critical current density.

4 Conclusions

Measurements on persistent current multipole fields have been performed for a large number of superconducting dipole and quadrupole magnets. The data show good internal consistency and reproducibility. A calculation of eddy current effects based on the critical state model describes the experimental results with remarkable success. The remaining discrepancies may be attributed partly to imprecise knowledge of the critical current densities at low magnetic fields but also reflect the experimental errors and the limits of the model.

In conclusion, the eddy current model presented in this paper leads to a rather accurate description of the field distortions caused by persistent currents in superconducting filaments. The qualitative and almost quantitative understanding of these effects is useful for the HERA machine and probably also for other future accelerators with superconducting magnets.

Acknowledgements. We thank the members of the magnet measuring group for their efforts in data taking and the staff of the refrigerator plant for the regular supply with liquid helium to operate the magnet test facility.

References

1. For a recent review of the HERA collider see B.H. Wiik: Proceedings of the XXIV International Conference on High Energy Physics, München 1988
2. K.-H. Mess, P. Schmüser: DESY report HERA 89-01 (1989) and Proceedings of the Course on Superconductivity in Particle Accelerators, Hamburg, CERN yellow report 89-04 (1989)
3. R.W. Hanft et al.: Contribution to the 1988 Conference on Applied Superconductivity
4. C. Daum et al.: IEEE Trans. Mag. 24 (1988) 1377; DESY report HERA 89-09 (1989)
5. R. Brinkmann, F. Willeke: DESY report HERA 88-08 (1988)
6. M.A. Green: IEEE Trans. Nucl. Sci. 18 (1971) 664

7. M.A. Green: LBL report LBID-1343 (1987)
8. J.-L. Duchateau: Department SATURNE internal report SEDAP/72-109 (1972)
9. J. Perot: Saclay Internal report SUPRA/80-37 HERA (1980)
10. H. Brück et al.: to be published
11. G. Hase et al.: DESY report HERA 87-23 (1987)
12. S. Wolff: DESY report 87-116 (1987); P. Schmüser, Proceedings of the Oregon APS Meeting, 1985
13. A. Auzolle et al.: Contribution to the ICFA Workshop on Superconducting Magnets and Cryogenics, Brookhaven, 1986, BNL report 52006
14. M.N. Wilson: Superconducting magnets. Oxford: Clarendon Press, 1983
15. D. ter Avest, L.J.M. van de Klundert: University of Twente internal report, 1989
16. A.K. Ghosh et al.: IEEE Trans. Mag. 23 (1987); M.A. Green: LBL-report 23823 (1987)
17. C.P. Bean: Phys. Rev. Lett. 8 (1962) 250; Y.B. Kim, C.F. Hempstead, A.R. Strnad: Phys. Rev. Lett. 9 (1963) 306
18. A.K. Ghosh, W.B. Sampson: private communication, see also A.K. Ghosh et al.: IEEE Trans. Mag. 21 (1985) 328